An advanced fully 3D OSEM reconstruction for positron emission tomography[*]

YUN Ming-Kai(贠明凯)[1,2]   LIU Shuang-Quan(刘双全)[1,2]   SHAN Bao-Ci(单保慈)[1;1)]   WEI Long (魏龙)[1]

[1] Key Laboratory of Nuclear Analytical Techniques, Institute of High Energy Physics, CAS, Beijing 100049, China

[2] Graduate University of Chinese Academy of Sciences, Beijing 100049, China

Abstract A fully 3D OSEM reconstruction method for positron emission tomography (PET) based on symmetries and sparse matrix technique is described. Great savings in both storage space and computation time were achieved by exploiting the symmetries of scanner and sparseness of the system matrix. More reduction of storage requirement was obtained by introducing the approximation of system matrix. Iteration-filter was performed to restrict image noise in reconstruction. Performances of simulation data and phantom data got from Micro-PET (Type: Epuls-166) demonstrated that similar image quality was achieved using the approximation of the system matrix.

Key words 3D OSEM, PET, symmetries, sparse matrix

PACS 25.30.Hm 87.80.-y, 87.85.-d

1 Introduction

Statistical iteration reconstruction method has been widely used in position emission tomography (PET) and other imaging techniques. The significant merit of statistical iteration reconstruction method is that it can achieve excellent image quality and quantitative analysis characteristic compared with that of filtered back projection (FBP) [1] since a more accurate model can be utilized to map the image space to the projection data [2]. Several statistical image reconstruction algorithms such as maximum likelihood expectation maximization (MLEM) [3], row-action maximum likelihood algorithm (RAMLA) [4] and ordered subset expectation maximization (OSEM) [5] have been developed in the past decades. However, the huge storage requirement and time consuming are the challenges of these methods especially in three-dimension (3D) mode. To solve these problems a hybrid approach [6] has been developed. In this approach the 3D sinogram is first rebinned to two-dimension (2D) data, and then each 2D sinogram is reconstructed by 2D techniques such as FBP and 2D-OSEM. This hybrid approach has considerably reduced the data size and time consumption. However, in this method the projection process is modeled as line integral theoretically [7], this assumption may not be suitable for delicate PET in the case of high resolution. In addition, the statistical properties of the rebinned data do not obey the Poisson distribution which is the foundation of MLEM and OSEM. Another way to solve the storage problem is to calculate the system matrix on the fly. But in practice, it's a waste of computing resources to calculate the system matrix in the reconstruction.

With the development of computer science, the memory and calculating ability have been greatly improved. Together with some tips, such as scanner symmetries and sparseness of system matrix [8, 9], 3D OSEM has recurred with the concern of people. In this work, an advanced fully 3D OSEM reconstruction using pre-computed system matrix based on symmetries and sparse matrix technique is depicted. The system matrix is divided into two parts: index matrix and probability matrix. These two matrixes are further compressed by exploiting the symmetries of the scanner and sparse matrix technique. In addition, considering the characters of the data organi-

zation of PET, we have introduced approximation of the probability matrix to further reduce the storage. Thousands times of reduction in storage have been achieved. The advanced fully 3D OSEM reconstruction method could be easily performed on an ordinary personal computer. To evaluate the new method, the image quality and convergence rate using the approximation system matrix are compared with that using normal system matrix.

2 Methods and materials

The formula of OSEM algorithm [5] is

$$f^{(k)}(i) = \frac{f^{(k-1)}(i)}{\sum\limits_{j\in s_n} p(i,j)} \sum_{j\in s_n} \frac{p(i,j)d(j)}{\sum\limits_{i'} p(i',j)f^{(k-1)}(i')}, \quad (1)$$

where $d(j)$ is the jth projection, $f^{(k)}(i)$ is the ith element of the reconstructed image at the kth iteration, $p(i,j)$ is the element of system matrix which represents the probability of an event in pixel i being detected by line of response (LOR) j and S_n is the nth subset of projection data.

2.1 System matrix

System matrix $P = \{p(i,j)\}$ models the relationship between the reconstructed image and the projection data. In this matrix, many effects can be contained, such as the geometric sensitivity, linear attenuation, intrinsic detector efficiency, positron range, inner crystal penetration and so on. In this work the solid angle of the two crystals of each LOR suspending to the image pixel is treated as the element of system matrix. Owing to the large number of LORs and image pixels in 3D pattern, the size of system matrix is huge. Taking the Micro-PET scanner (Type: Eplus-166) as an example (Table 1), there are $127\times256\times528$ LORs. The image pixel number is $128\times128\times64$. The full system matrix will have $127\times256\times528\times128\times128\times64=1.8\times10^{13}$ elements in this case. If each element is represented by float number, the total storage requirement will be more than 65T bytes. This is a kittle obstacle for the using of 3D OSEM reconstruction.

2.2 Sparseness and symmetries

In fact, the values of most elements of the system matrix are zero. It is clear that $p(i,j)=0$ when there is no cross section between the image pixel i and LOR j. Therefore the matrix of positron tomography scanner is highly sparse. Only the nonzero elements will be available in implementation and need to be

stored. By exploiting the sparse matrix technique, the nonzero elements are extracted from the original system matrix and indexed in a compressed pattern. Just the nonzero elements are used in the projection and back-projection. Thus thousands' times of reduction of storage space and calculation time consumption can be achieved.

The storage of the nonzero elements of the system matrix is still a problem because of the huge number of the LORs in 3D mode. Taking advantage of the symmetries of the scanner provides a promising way. Disregarding the attenuation and any other physical effects of the system matrix, in-plane symmetries and axial symmetry can be introduced [8, 9]. According to the in-plane symmetries, we need only to calculate and store the first quarter of the system matrix correlated to LORs range $[0, \pi/2)$. The other three quarters can be gotten from the first quarter by rotating the pixel index of $\pi/2$, π and $3\pi/2$. Fig. 1 illustrates the LORs of 0 (vertical lines) and $\pi/2$ (horizontal lines). As to the axial symmetry, the projection data can be divided into several individual segments according to the ring difference number $(0, 1, 2, \cdots, 31)$. Each segment contains many slices at different axial positions. Only the part of system matrix correlated to the first slice of each segment is needed and the other parts can be calculated by translating the axial index (Fig. 1(b)). In this way, 4-fold in-plane symmetries and 16 equivalent axial symmetries are achieved. After using the sparse matrix and symmetries techniques the full system matrix is compressed to about 6.7×10^7 elements.
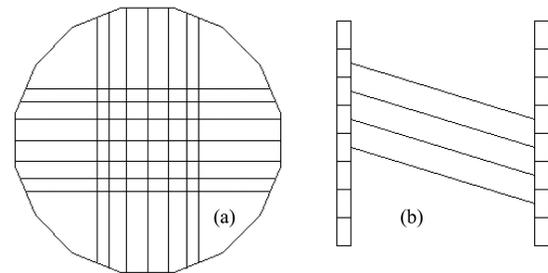

Fig. 1. Schematic representation of symmetries, (a) in-plane symmetries, (b) axial symmetry.

2.3 Further reduction of system matrix

It is still difficult to load the whole system matrix in memory after using sparse matrix technique and symmetries. Further reduction of system matrix should be introduced. Since the large ring difference corresponds to the obvious depth of interaction (DOI) effect, orientation error will happen when the data of

large ring difference number are used. The practiced ring difference number (RD) in reconstruction should counterpoise the DOI effect and the statistic noise. In this work, only the data correlated to small ring difference number are used to avoid orientation error and the statistic character is improved enough. That is to say the differences between the system matrix corresponds to different RD are very small. We can use the probability matrix of one slice instead of the entire matrix. The experiential RD of 10 is adopted in Eplus-166 3D OSEM reconstruction in static inspection, which means the polar angle of the LORs is less than 8°. We use the probability matrix corresponding to RD Number 5 empirically instead of the entire probability matrix corresponding to all the 11 different RDs ranging from 0–10. Nearly a half more reduction of the storage is achieved on the basis of sparse matrix and symmetries.

2.4   Evaluation methods and data

To evaluate the performance of the advanced method, we use the experiment data got from the Micro-PET scanner to test the spacial resolution at different axial positions. Simulation data from Geant4 Application for Tomographic Emission (GATE) are also introduced to evaluate the convergent rate, contrast recovery and signal to noise ratio. For the Micro-PET scanner Eplus-166, the first delicate PET scanner for small animals designed by Institute of High Energy Physics, Chinese Academy of Sciences (Table 1), 16 modules are arranged in equilateral polygon, providing 32 crystal rings with an axial length of 64 mm and 166 mm face to face distance of opposite crystals. Each module has two blocks which consists of a 16×16 array of Cerium-doped Lutetium Yttrium Orthosilicate (LYSO) crystal elements coupled to a position-sensitive photomultiplier. Each crystal element has the size of 1.9 mm×1.9 mm×10 mm. Reflective materials are used to improve the light collection efficiency, and the results in crystal pitch of 2.0 mm×2.0 mm in both the axial and transverse directions. Each crystal can be coincident with 127 crystals in opposition in each ring. The transverse field of view (FOV) is 110 mm. The maximum ring difference of 31 is accepted. No angle mashes to preserve the spatial resolution.

A miniature Derenzo phantom filled with ^{18}F-FDG is imaged to measure the spatial resolution of the two methods at different axial positions. The hot rod diameters of the miniature Derenzo phantom are 1.4 mm, 1.6 mm, 1.9 mm, 2.2 mm, 2.5 mm and 3.0 mm. The center to center distance between

rods is twice the hot rod diameter. Random events are subtracted from prompt events through the delayed timing window technique. The negative values introduced by subtraction are set to zero. The reconstructed image pixel size is 0.5 mm×0.5 mm×1 mm, and the pixel number is 180×180×64. The subset number is 16, and the iteration number is 2.

Table 1.   Characters of Micro-PET Eplus-166.

rings number	32
crystals number per ring	256
face to face distance of opposite crystals	166 mm
transverse FOV	110 mm
axial FOV	64 mm
maximum ring difference	31
transaxial angles per sinogram	512(3D) 256(2D)
LORs number per angle	127
slices number per sinogram	528
crystal size	1.9 mm × 1.9 mm × 10 mm
crystal pitch	2.0 mm × 2.0 mm

A thin column and cube are simulated (about $1.4×10^7$ coincidences) using GATE, which is a toolkit package allowing to simulate the emission and detection processes. The parameters of the simulated scanner are the same as those of Eplus-166. The thin column has the size of 10 mm in diameter and 2 mm in height, filled with 0.5 mCi ^{18}F solution. The center of this column is located at (10 mm, 10 mm, 0 mm). The cube has the size of 10 mm×10 mm×2 mm, filled with 2 mCi ^{18}F solution. And its center is located at (−15 mm, −5 mm, 0 mm). The image pixel size used in the reconstruction is 0.5 mm×0.5 mm×1 mm and the image size is 128×128×64. The subset number is 16. Each subset has 16 angles projection data. The regions of interesting (ROI) of 8×8×4 pixels are chosen in the central adjacent 4 slices to cover the whole source along the axial direction for the contrast and noise to signal ratio calculation.

All the data are acquired in 3D mode with the maximum ring difference of 31. But in reconstruction the RD of 10 is used. No scatter and attenuation corrections are implemented in both simulation and experiment. In order to regularize the reconstructed image, iteration-filter is introduced in the reconstruction. A 3×3 spatial Gaussian filter with standard deviation of 0.7 is implemented after each full-iteration.

3   Results

3.1   Simulation data

According to the activity of the ^{18}F solution filled

in these two sources, the contrast ratio of cube to column in this case should be π. Fig. 2 plots the contrast ratio (CR) of cube to column vs. iteration number using full system matrix and approximation matrix

separately. Fig. 3 and Fig. 4 present the signal to noise ratio (SNR) of the cube and column separately. It can be seen that nearly the same convergent rate is achieved in both methods. The approximation
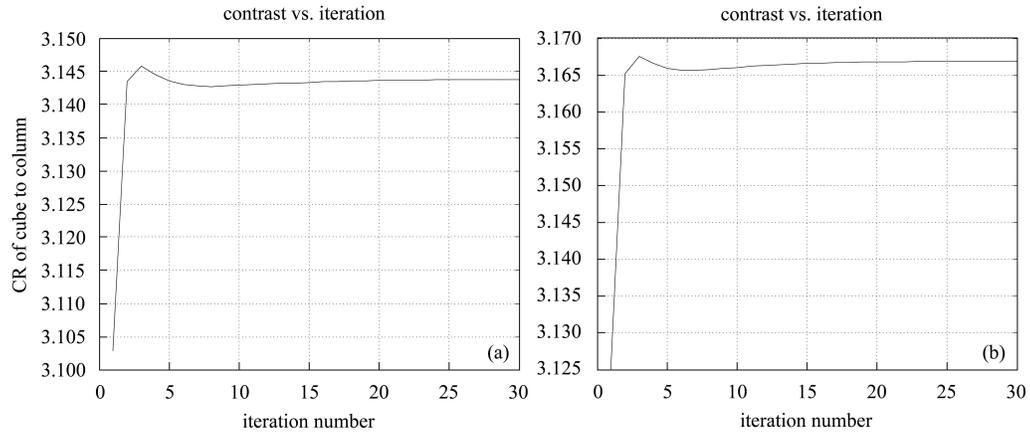
Fig. 2. CR of cube to column vs. iteration number, (a) full matrix (b) approximation matrix.
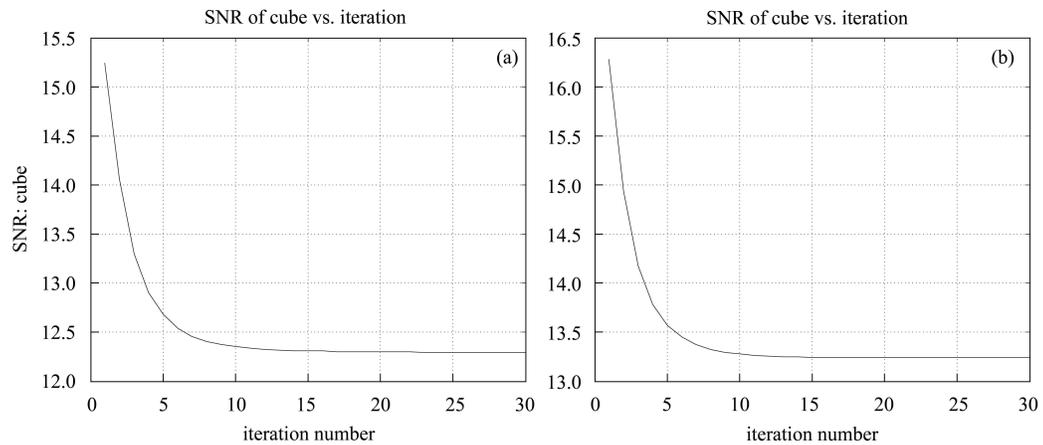
Fig. 3. SNR of cube vs. iteration number, (a) full matrix (b) approximation matrix.
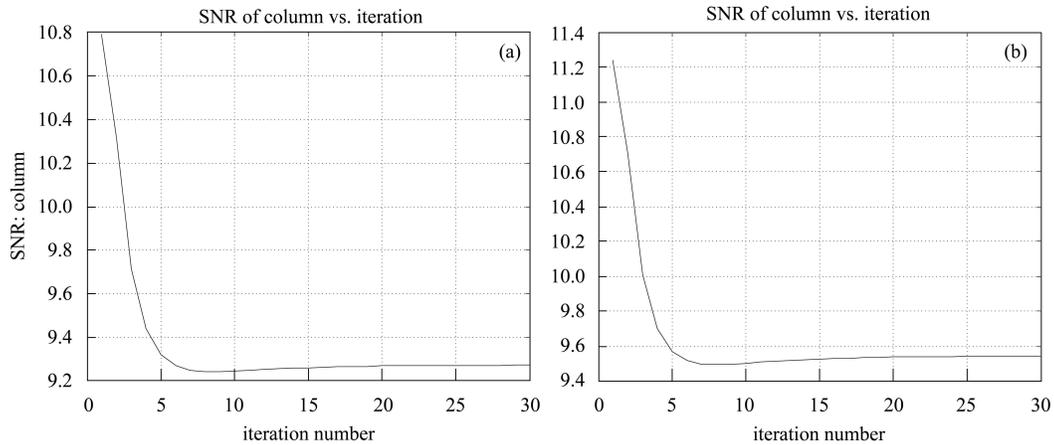
Fig. 4. SNR of column vs. iteration number, (a) full matrix (b) approximation matrix.

method can obtain a little higher signal to noise ratio, which is important in low statistical case. However, the contrast ratio of the cube to column has a little warp.

3.2   Experiment data

Figures 5 and 6 show the 48th slice and the 44th slice of the reconstructed image which correspond to the center and the end of the phantom. The two figures indicate that similar results of special resolution are achieved using the above two methods at different axial positions. The only difference is the artifact distribution. In the full matrix method, the artifacts are concentrated on the central region of the image. In contrast, in the approximation method the artifacts spread around the hot rods.
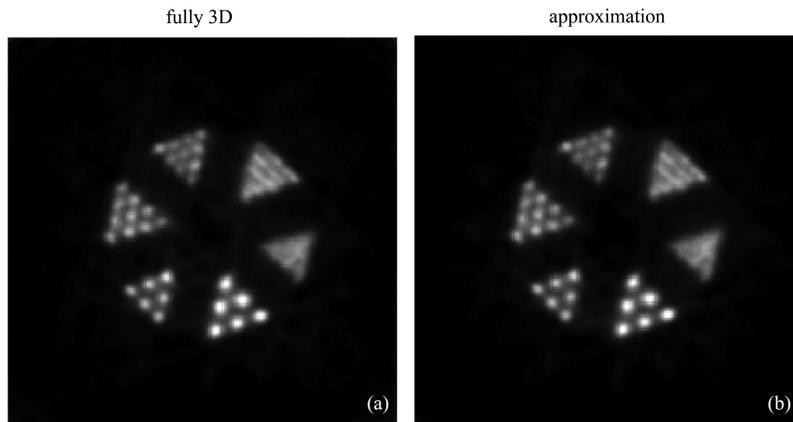

Fig. 5.   Reconstructed image of the Derenzo phantom (48th slice), (a) full matrix (b) approximation matrix.
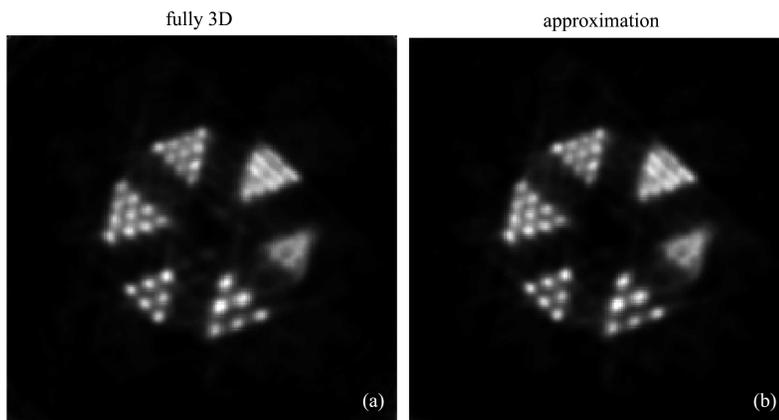

Fig. 6.   Reconstructed image of the Derenzo phantom (44th slice), (a) full matrix (b) approximation matrix.

3.3   Multithread implementation

Multithread technique is exploited to further shorten the reconstruction time. A multithread version of 3D OSEM has been implemented on an 8-core processor (two 4-core processors). One full-iteration for a position (projection data size $127 \times 256 \times 528$) takes about 69 seconds on Intel 8-core 2.0 GHz processor compared with 295 seconds on the Intel single core 2.0 GHz processor. If the maximum ring difference (RD) used in reconstruction is 10, one full-iteration takes only about 24 seconds on the 8-core processor. Owing to the time consumption of I/O stream and control instruction, about 4 times acceleration is achieved. This is different from the case of cores. However, it fulfills the requirement of clinic or experiment.

4   Discussion

3D data acquisition becomes popular in modern PET scanner for increasing sensitivity. But the system matrix goes into a tremendously huge size accordingly. Accurate system matrix results in better

image quality [10, 11]. Generally, the accurate system matrix will be accompanied with complex computing and large storage. Fortunately the system matrix used in statistical reconstruction is usually very sparse due to the fact that each LOR covers a finite number of image pixels which is much smaller than the pixel number of the whole FOV. In-plane symmetries and axial symmetry of PET scanner, in addition to rotational symmetry [8, 12] disregarding the display of reconstructed image, can be exploited to compress the system matrix effectively for storage and loading.

Although great savings can be achieved using sparse matrix technique and symmetries, it is still a challenge to load the system matrix in memory. It is an impediment in the reconstruction to read the matrix from disk time after time. Approximation provides further reduction of the system matrix. The storage requirement can be reduced ulteriorly on the basis of sparse matrix technique and symmetries.

Since to what degree the image quality is affected by the fluctuation of system matrix is still an open issue [13], the convergent rating, contrast recovery and signal to noise ratio using approximation matrix are evaluated in this work. The performances show that little change in the magnitude of the system matrix may not result in obvious decrease of the image quality, at least in some regions. To validate the applicability of the approximation in system matrix contrast recovery and signal to noise ratio departure from the center along axial will be tested in future work. As to the spacial resolution, similar exhibition can be gotten using approximation system matrix with that of using full matrix at different axial positions.

References

1 Chatziioannou A, QI J, Moore A et al. IEEE Trans. Med. Imag., 2000, **19**(5): 507–512
2 Terstegge A, Weber S, Herzog H et al. IEEE Nuclear Science Symposium Conference Record, 1996, **3**: 1603–1607
3 Shepp L A, Vardi Y. IEEE Trans. Med. Imag., 1982, **MI-1**(2): 113–122
4 Browne J, De Pierro A R. IEEE Trans. Med. Imag., 1996, **15**(5): 687–699
5 Hudson H M, Larkin R S. IEEE Trans. Med. Imag., 1994, **13**(4): 601–609
6 Defrise M, Kinahan P E, Townsend D W et al. IEEE Trans. Med. Imag., 1997, **16**(2): 145–158
7 LIU X, Comtat C, Michel C et al. IEEE Trans. Med. Imag., 2001, **20**(8): 804–814
8 Kaufman L. IEEE Trans. Med. Imag., 1987, **MI-6**(1): 37–51
9 Johnson C A, YAN Y, Carson R E et al. IEEE Trans. Nucl. Sci., 1995, **42**(4): 1223–1227
10 Fazendeiro L, Ferreira N C, Blanco A et al. IEEE Nuclear Science Symposium Conference Record, 2004, **4**: 2511–2515
11 Alessio A M, Kinahan P E, Lewellen T K. IEEE Trans. Med. Imag., 2006, **25**(7): 828–837
12 Scheins J, Herzog H. 9th International Meeting on Fully Three-Dimensional Image Reconstruction in Radiology and Nuclear Medicine. 49–51
13 QI J, Huesman R H. Phys. Med. Biol., 2005, **50**: 3297–3312